Towards self-adaptive efficient global optimization

Cite as: AIP Conference Proceedings **2070**, 020056 (2019); https://doi.org/10.1063/1.5090023 Published Online: 12 February 2019

Hao Wang, Michael Emmerich, and Thomas Bäck

ARTICLES YOU MAY BE INTERESTED IN

Weighted ensembles in model-based global optimization AIP Conference Proceedings **2070**, 020003 (2019); https://doi.org/10.1063/1.5089970

The R2 indicator: A study of its expected improvement in case of two objectives AIP Conference Proceedings **2070**, 020054 (2019); https://doi.org/10.1063/1.5090021

Combining local surrogates and adaptive restarts for global optimization of moderately expensive functions

AIP Conference Proceedings 2070, 020048 (2019); https://doi.org/10.1063/1.5090015

AP Conference Proceedings



Enter Promotion Code PDF30 at checkout

AIP Conference Proceedings 2070, 020056 (2019); https://doi.org/10.1063/1.5090023

2070, 020056

View Onlin

© 2019 Author(s).

Get 30% off all

print proceedings!

Towards Self-Adaptive Efficient Global Optimization

Hao Wang^{1,a)}, Michael Emmerich^{1,b)} and Thomas Bäck^{1,c)}

¹LIACS, Leiden University, Niels Bohrweg 1, 2333CA Leiden, Netherlands

^{a)}Corresponding author: h.wang@liacs.leidenuniv.nl ^{b)}m.t.m.emmerich@liacs.leidenuniv.nl ^{c)}t.h.w.baeck@liacs.leidenuniv.nl

Abstract. In this paper, it is proposed to dynamically control the trade-off between exploration and exploitation for the efficient global optimization algorithm. To achieve this, we use the so-called Moment-Generating Function of Improvement criterion, in which an additional parameter, called "temperature", is introduced to smoothly control the exploration/exploitation balance. It is proposed to adapt the temperature using two approaches: 1) a success-rate based mechanism 2) a self-adaptive algorithm where multiple different temperatures are used to generate new points. The temperature related to the best point is then selected for the next iteration. The self-adaptive algorithm is validated on two multi-modal functions and the result shows that the adaptive temperature mechanism speeds up the convergence rate of EGO, compared to the fixed temperature setting.

MOMENT-GENERATING FUNCTION OF IMPROVEMENT

In this paper, we consider the following real-valued objective function: $f : S \subseteq \mathbb{R}^d \to \mathbb{R}$, which is subject to minimization. The well-known Efficient Global Optimization algorithm [1], starts with sampling an initial design of points: $X = \{\mathbf{x}^{(1)}, \mathbf{x}^{(2)}, \dots, \mathbf{x}^{(n)}\} \subseteq S$. The corresponding objective values are denoted as $Y = \{y^{(1)}, y^{(2)}, \dots, y^{(n)}\} = \{f(\mathbf{x}^{(1)}), f(\mathbf{x}^{(2)}), \dots, f(\mathbf{x}^{(n)})\}$. Then, a Gaussian process prior is assumed on f and the posterior Gaussian process can be given [2]: $f(\mathbf{x}) \mid Y \sim \mathcal{N}(\hat{f}(\mathbf{x}), s^2(\mathbf{x}))$, where \hat{f} is the approximation/estimate for f and s^2 quantifies the uncertainty of the approximation. Note that \hat{f} and s^2 depend on the choice of the prior on f. Please see [2] for details. To select promising points for the evaluation, it is common to balance \hat{f} with s^2 (and thus make trade-offs between exploration and exploitation), resulting in the so-called infill criterion. Moreover, some infill criteria explicitly control this trade-off, e.g., Generalization Expected Improvement (GEI) [3] and *Moment-Generating Function of Improvement* (MGFI) [4]. For the latter, our previous investigation shows that tuning down the exploration effect (using the cooling strategy) helps improving the performance of EGO on some highly multi-modal test functions [5]. In this paper, the goal is to generalize the prescribed cooling strategy to the dynamic online adaptation of the exploration/exploitation effect. Some infill-criteria are built on the statistical properties of the *improvement* over the current best function value: $I(\mathbf{x}) = \max\{0, f_{\min} - f(\mathbf{x})\}$, where $f_{\min} = \min Y$. Taking the posterior process of f into account, $I(\mathbf{x}) \mid Y$ has a rectified Gaussian distribution [4]. The so-called *Moment-Generating Function of Improvement* (MGFI) is [4, 5]:

$$\mathcal{M}(\mathbf{x};t) = \Pr(I(\mathbf{x}) > 0 \mid Y) + \frac{t}{e^{t}} \mathbb{E}\{I(\mathbf{x}) \mid Y\} + \frac{t^{2}}{2!e^{t}} \mathbb{E}\{I^{2}(\mathbf{x}) \mid Y\} + \frac{t^{3}}{3!e^{t}} \mathbb{E}\{I^{3}(\mathbf{x}) \mid Y\} + \cdots$$
$$= \Phi\left(\frac{f_{\min} - \hat{f}'(\mathbf{x})}{s(\mathbf{x})}\right) \exp\left(\left(f_{\min} - \hat{f}(\mathbf{x}) - 1\right)t + \frac{s^{2}(\mathbf{x})}{2}t^{2}\right), \tag{1}$$

where $\hat{f}'(\mathbf{x}) = \hat{f}(\mathbf{x}) - s^2(\mathbf{x})t$ and an additional parameter $t \in \mathbb{R}_{\geq 0}$ ("temperature") is introduced to balance exploration with exploitation. When t goes up, \mathcal{M} tends to reward points with a high uncertainty as higher moments of $I(\mathbf{x})$ are dominating the lower ones. When t decreases, lower moments contribute more to \mathcal{M} and thus points with less uncertainty are preferred. MGFI is closely related to the so-called Generalization Expected Improvement (GEI) [3], defined as GEI($\mathbf{x}; g$) = $\mathbb{E}\{I^g(\mathbf{x}) \mid Y\}$. Instead of specifying a moment as in GEI, MGFI aggregates several consecutive moments and therefore exhibits a smoother change when scaling the temperature t.

> Proceedings LeGO – 14th International Global Optimization Workshop AIP Conf. Proc. 2070, 020056-1–020056-4; https://doi.org/10.1063/1.5090023 Published by AIP Publishing. 978-0-7354-1798-4/\$30.00

SELF-ADAPTATION PROPOSAL

In this section, it is proposed to further investigate the possibility of devising an *adaptive* mechanism for *t*. Firstly, it is important to see how the temperature links to the step-wise progress and success rate of EGO. Note that, in practice, the newly generated location is obtained by applying a *stochastic optimization algorithm* (e.g., evolution strategies [6]) on the problem arg max_{x∈S} $\mathcal{M}(x; t)$. As a consequence, the new location is also stochastic and we define the *empirical* step-wise progress *c* and success rate *p* as:

$$c(t) = \mathbb{E}\left\{I(\mathbf{x}') \mid \mathbf{x}' = \operatornamewithlimits{argmax}_{\mathbf{x} \in S} \mathcal{M}(\mathbf{x}; t)\right\}, \qquad p(t) = \Pr\left\{I(\mathbf{x}') > 0 \mid \mathbf{x}' = \operatornamewithlimits{argmax}_{\mathbf{x} \in S} \mathcal{M}(\mathbf{x}; t)\right\},$$

where arg max indicates the (stochastic) asymptotic maximizer of the optimization problem therein. The empirical progress and success rate should not be confused with the expected improvement (EI) and probability of improvement (PI): the randomness in EI/PI comes from the underlying Gaussian process model. It is proposed to control the temperature online such that the empirical progress c(t) is maximized, i.e., $t^* = \arg \max c(t)$. However, this cannot be directly implemented: the graph of c(t) is typically non-monotonic (Fig. 1, right) and therefore it is not possible to determine whether t should be increased or decreased. Alternatively, the well-known adaptation mechanism from the evolution strategy, called 1/5-success rule [6], is adopted to control parameter t in the following manner. t is dynamically modified such that the measured success rate p(t) approximately equals a target rate p_{target} : t is increased when $p(t) > p_{target}$ and vice versa. This adaptation approach is summarized in Alg. 1. As for the target success rate, it is possible to use the corresponding success rate when the progress is maximized, namely $p_{target} = p(t^*)$, $t^* = \arg \max c(t)$. Such a target success rate is illustrated in Fig. 1, where success rate at the peak of c(t) is approximately 0.8. However, according to other experiments conducted (not shown here), the target success obtained in this manner depends on the choice of objective function and the number of data points. Therefore there is no general setting for p_{target} .

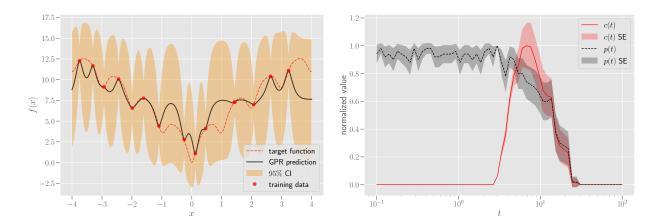


FIGURE 1. Left: on a 1-D *Ackley function* (red dashed curve), 15 points are sampled uniformly (red dots), on which a Gaussian process regression models (black curve) is trained. **Right**: the empirical progress c(t) (red curve) and success rate p(t) (black curve) are measured by varying t from 10^{-1} to 10^2 . The standard error (SE) of the measurement is shown as the shade area.

The second adaptation mechanism is based on the so-called *self-adaptation* that is original proposed in evolution strategies [6]. This approach is listed in Alg. 2. Essentially, prior to the maximization of \mathcal{M} , λ temperature mutations are generated using a log-normal distribution (line 8). Then λ new points are obtained by maximizing \mathcal{M} with all temperature mutations: $t_i \leftarrow t \exp(\tau \mathcal{N}(0, 1)), \mathbf{x}'_i \leftarrow \arg \max_{\mathbf{x} \in S} \mathcal{M}(\mathbf{x}; t_i)$, where τ controls the range of temperature mutation. In this paper, we simply adopt the setting $\tau = 1/\sqrt{d}$ from self-adaptive evolution strategies [6]. Note that such an approach also allows for the parallel execution of points [7]. After evaluating the new points, the temperature mutation corresponding to the best point is selected as the new temperature (line 16, 17). Compared to Alg. 1, this approach does not require the user to set the problem-dependent parameter p_{target} and thus should be more easily applicable.

Algorithm 1 EGO with success rate control		Algorithm 2 $(1, \lambda)$ -self-adaptive EGO	
1: procedure (1 + 1)-EGO(<i>d</i> , <i>f</i> , S , <i>p</i> _{target})		1: procedure (1, λ)-self-adaptive-ego(d, λ, f, S)	
2:	$c \leftarrow 0, \ \alpha \in [0.817, 1)$	2:	$\tau \leftarrow 1/\sqrt{d}$
3:	$\mathbf{s} \leftarrow $ an empty array of length 10 d	3:	sample the initial design $X = {\mathbf{x}_1, \dots, \mathbf{x}_n} \subseteq S$
4:	sample the initial design $X = {\mathbf{x}_1, \ldots, \mathbf{x}_n} \subseteq S$	4:	evaluate $Y \leftarrow \{f(\mathbf{x}_1), f(\mathbf{x}_2), \dots, f(\mathbf{x}_n)\}$
5:	evaluate $Y \leftarrow \{f(\mathbf{x}_1), f(\mathbf{x}_2), \dots, f(\mathbf{x}_n)\}$	5:	fit the Gaussian process model on X, Y.
6:	fit the Gaussian process model X, Y.	6:	while stopping criteria are not fulfilled do
7:	while the stop criteria are not fulfilled do	7:	for $i = 1 \rightarrow \lambda$ do
8:	$\mathbf{x}' \leftarrow \arg \max_{\mathbf{x} \in \mathbf{S}} \mathcal{M}(\mathbf{x}; t)$	8:	$t_i \leftarrow t \exp(\tau \mathcal{N}(0, 1))$
9:	$X \leftarrow X \cup \{\mathbf{x}'\}, Y \leftarrow Y \cup \{y'\}, y' \leftarrow f(\mathbf{x}')$	9:	$\mathbf{x}'_i \leftarrow \arg \max_{\mathbf{x} \in \mathbf{S}} \mathcal{M}(\mathbf{x}; t_i)$
10:	$k \leftarrow c \mod 10d$,	10:	$y'_i \leftarrow f(\mathbf{x}'_i)$
1:	$s_k \leftarrow 1$ if $f(\mathbf{x}') < f_{\min}$; otherwise 0	11:	end for
12:	if $c \mod d = 0$ then	12:	$X \leftarrow X \cup \{\mathbf{x}'_1, \dots, \mathbf{x}'_{\lambda}\}, Y \leftarrow Y \cup \{y'_1, \dots, y'_{\lambda}\}$
13:	$p \leftarrow \sum_{i=1}^{10d} s_i / 10d$	13:	choose k such that $y'_k = \min\{y'_1, \dots, y'_k\}$
14.	$t \leftarrow \begin{cases} \alpha t & \text{if } p < p_{\text{target}}, \\ t/\alpha & \text{if } p > p_{\text{target}} \end{cases}$	14:	$t \leftarrow t_k$
14:	$t \leftarrow \begin{cases} t/\alpha & \text{if } p > p_{\text{target}} \end{cases}$	15:	fit the Gaussian process model on X, Y
15:	end if	16:	end while
16:	fit the Gaussian process model on X, Y	17: e	nd procedure
17:	$c \leftarrow c + 1$		
18:	end while		
19: end procedure			
0.6-	fixed	7 —	I TITI I

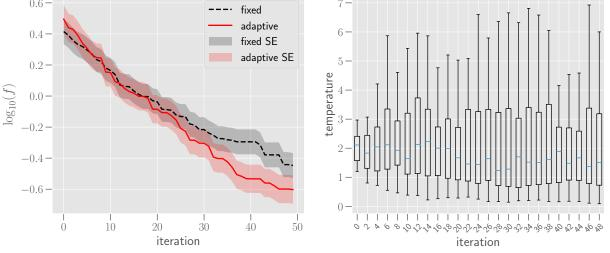


FIGURE 2. Left: on a 2-D *Ackley function*, the measured convergence rate of the self-adaptive EGO (the red curve) is compared to an EGO with the fixed temperature setting: t = 2 (the black curve). The values are averaged over 30 runs. **Right**: the boxplot of temperatures (the median is indicated by the blue bar).

EMPIRICAL INVESTIGATION AND DISCUSSION

In this section, we test Alg. 2 on two multi-modal functions: the well-known *Ackley* function and the BBOB f22 function. For the experiment, the size of the initial design of experiment is $10 \times d$ and λ is set to 5. The initial temperature t_0 is set to 2. For the Ackley function, 50 iteration is conducted and $18 \times d$ iterations are performed for the BBOB f22 function ($100 \times d$ function evaluations in total). For the settings of the Gaussian process model, the Matérn 3/2 kernel is used throughout the experiment. As for the maximization of infill criteria, the L-BFGS algorithm

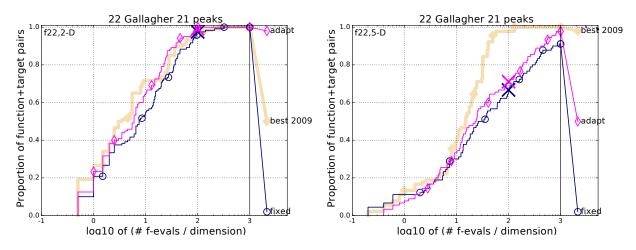


FIGURE 3. Empirical cumulative distribution of the number of objective function evaluations divided by dimension (2-D (**left**) and 5-D (**right**)). The targets are chosen from $10^{[-8.2]}$ such that the bestGECCO2009 artificial algorithm just did not reach them within a given budget of $k \times \text{DIM}$, with $k \in \{0.5, 1.2, 3, 10, 50\}$. The "best 2009" line corresponds to the best ERT observed during BBOB 2009 for each selected target.

with restarting heuristic (20 restarts) is applied with $50 \times d$ evaluation budget. The results on the Ackley function are shown in Fig. 2. In the left sub-figure, the convergence of the self-adaptive EGO is compared to an EGO with the fixed temperature setting: t = 2. The measured convergence is averaged over 30 independent runs. It is clear that the selfadaptive EGO outperforms the fixed-temperature EGO from 30 iteration onwards. The adaptation of the temperature is depicted as boxplots on the right sub-figure. In each iteration, the temperatures shows a quite large dispersion, which implies that the adaptation mechanism in Alg. 2 is not stable. This could result from the usage of a small number of point ($\lambda = 5$). Moreover, the median of temperatures (blue bars) gradually decreases from iteration 20, reinforcing the exploitative effect. We speculate that this is the cause of comparisons on the convergence. In Fig. 3, the **empirical cumulative distribution functions** (ECDFs) of the running time (function evaluations) are shown for the BBOB f22function: when d = 2, the ECDF of the self-adaptive EGO is significantly better that of the fixed-temperature EGO. Such an advantage still holds when d = 5.

For future work, it is necessary to test the proposed approaches on more test functions and in higher dimensions. In addition, it is important to take a simple objective function (e.g., the sphere function) to analyze the relation between the empirical progress/success rate to the number of data points and the quality of the underlying Gaussian process model.

REFERENCES

- [1] J. Močkus, *Bayesian approach to global optimization: theory and applications*, Vol. 37 (Springer Science & Business Media, 2012).
- [2] C. Rasmussen and C. Williams, *Gaussian Processes for Machine Learning*, Adaptative computation and machine learning series (University Press Group Limited, 2006).
- [3] M. Schonlau, W. J. Welch, and D. R. Jones, "Global versus Local Search in Constrained Optimization of Computer Models," (Institute of Mathematical Statistics, 1998), pp. 11–25.
- [4] H. Wang, B. van Stein, M. Emmerich, and T. Bäck, "A New Acquisition Function for Bayesian Optimization based on the Moment-Generating Function," in *Systems, Man, and Cybernetics (SMC), 2017 IEEE International Conference on* (IEEE, 2017), pp. 507–512.
- [5] H. Wang, M. Emmerich, and T. Bäck, "Cooling Strategies for the Moment-Generating Function in Bayesian Global Optimization," in *Evolutionary Computation (CEC), 2018 IEEE Congress on* (IEEE, 2018).
- [6] T. Bäck, *Evolutionary Algorithms in Theory and Practice: Evolution Strategies, Evolutionary Programming, Genetic Algorithms* (Oxford University Press, Oxford, UK, 1996).
- [7] F. Hutter, H. H. Hoos, and K. Leyton-Brown, "Parallel Algorithm Configuration," in *Proceedings of the* 6th International Conference on Learning and Intelligent Optimization, LION'12 (Springer-Verlag, Berlin, Heidelberg, 2012), pp. 55–70.